Materials Science in Semiconductor Processing 66 (2017) 62–68

Contents lists available at ScienceDirect

Materials Science in Semiconductor Processing

journal homepage: www.elsevier.com/locate/mssp

Effects of graphite on the synthesis of 1-D single crystal In_2O_3 nanostructures at high temperature

Fatma Nur Tuzluca[a,d,*], Yasar Ozkan Yesilbag[a,d], Tuba Akkus[a], Mehmet Ertugrul[b,c,d]

[a] Department of Physics, Erzincan University, Erzincan 24100, Turkey
[b] Department of Electrical and Electronics Engineering, Ataturk University, Erzurum 25240, Turkey
[c] Department of Nanoscience and Nanoengineering, Ataturk University, Erzurum 25240, Turkey
[d] Nanoscience and Nanoengineering Application and Research Center, Ataturk University, Erzurum 25240, Turkey

ARTICLE INFO

Keywords:
Indium oxide
FESEM
HR-TEM
XRD
Photoluminescence
Graphite powder

ABSTRACT

This study investigated the effects of graphite powder on the growth mechanisms of one-dimensional (1-D) single-crystal indium oxide (In_2O_3) nanostructures. The study was conducted using a chemical vapor deposition (CVD) method at 1000 °C; In_2O_3 and graphite powder mixed with In_2O_3, with a weight ratio of 1:1, were used as the source material, while 2 nm-thick n-type silicon (100), coated with a gold catalyst, was used as a substrate. It was observed that nanostructures grew via a Vapor-Liquid-Solid (VLS) growth mechanism when only In_2O_3 was used, but grew via both VLS and Vapor-Solid (VS) growth mechanisms when graphite powder was used with the In_2O_3. The morphology and crystal structures of the nanostructures grown were investigated using X-Ray Diffraction (XRD), High Resolution Transmission Electron Microscopy (HR-TEM), Field Emission Scanning Electron Microscopy (FESEM) and Energy Dispersion X-Ray Spectroscopy (EDS). At room temperature (RT), all the nanostructures showed photoluminescence (PL) spectra at a wavelength of 367 nm in the UV-emission region and at wavelengths of 470 and 630 nm in the visible region.

1. Introduction

Indium oxide (In_2O_3) is an n-type semiconductor oxide that has a very wide band gap (Eg ≈3.6 eV). It is used as a transparent conductive oxide (TCO) due to its high permeability and conductivity characteristics [1–4]. **In_2O_3 is** also used in field emission [5], gas sensors [6] and solar cells [7] due to their morphologies, specific characteristics and potential applications in various nanodevices. For example, In_2O_3 structures used in toxic gas sensor applications have high sensitivity and selectivity characteristics, as well as very rapid response times [8,9].

In_2O_3 structures can be synthesized by numerous methods such as electrodeposition [10], a hydrothermal method [11,12], molecular beam epitaxy (MBE) [13] and chemical vapor deposition (CVD) [9,14–16]. The most widely used method among these is CVD. In this method, one-dimensional (1-D) single-crystal In_2O_3 nanostructures usually grow through VLS and VS growth mechanisms [4,17,18]. These growth mechanisms can be controlled by pressure and temperature differences [17,19,20], chemical media and reaction kinetics [21], thermodynamic behavior of the catalyst [22], the design of the growth media and composition of source materials. In other words, vapor concentration determines VLS and VS growth mechanisms. This phenomenon differentiates morphologies of In_2O_3 nanostructures, as a result of the fact that supersaturation ratios and the formation of crystal surfaces on nanostructures during the growth process depends on vapor concentration.

Because it is known that the properties of In_2O_3 nanostructures are highly dependent on their morphologies, it is useful to synthesize In_2O_3 nanostructures with different morphologies for a new generation of nanodevices. Therefore, this study—conducted using the CVD method—investigated the effects of the composition of source materials on the synthesis of 1-D single-crystal In_2O_3 nanostructures with different morphologies. **Previous studies found in other literature—that used only Indium (In) [5,23], or In_2O_3 [17], or graphite powder with In_2O_3 [6,9,18,24] as the source material—were conducted using separate experimental systems; however, this study—unlike others—is different in that it includes both In_2O_3, and graphite powder with In_2O_3, in the same experimental setup.** Hao et al. indicated in their study—where they used only In_2O_3 powder as the source material—that they obtained nanostructures with less density as a result of low vapor concentrations occurring at temperatures of 1350 °C and below. This is because the supersaturation ratio of Indium

---

* Corresponding author at: Department of Physics, Erzincan University, Erzincan 24100, Turkey.
E-mail address: ftuzluca@erzincan.edu.tr (F.N. Tuzluca).

http://dx.doi.org/10.1016/j.mssp.2017.04.007
Received 8 December 2016; Received in revised form 9 March 2017; Accepted 5 April 2017
1369-8001/

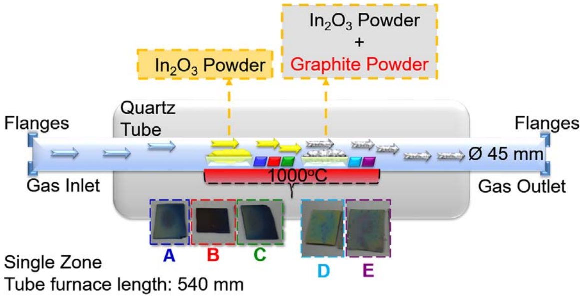

Fig. 1. Schematic of the experimental system.

oxide—which depends on its vapor concentration—is lower than that of indium at the same temperature [25]. Therefore, graphite powder was used to increase the vapor concentration of oxidized Indium by accelerating vaporization of In_2O_3 powder. In other words, in this study, the effects of vapor concentrations of Indium on the growth mechanisms of 1-D single-crystal In_2O_3 nanostructures are subject to the same growth temperature and pressure conditions.

2. Experimental

1-D single-crystal In_2O_3 nanostructures were synthesized in the experimental system indicated in Fig. 1. The system, whose operating temperature was set at 1000 °C, includes a single-zone, horizontal tube oven, a quartz tube with argon as the carrier gas (99.99% purity), and a vacuum pump with a vacuum reader connector. **In_2O_3 of 99.99% purity (trace metals basis) and graphite powder (Sigma-Aldrich)** mixed with In_2O_3 at a weight ratio of 1:1 was used as the source material. N-type silicon (100) was used as the substrate material. The substrate materials were first cleaned with acetone, methanol and deionized water in an ultrasonic bath for 10 min, respectively. Then, they were immersed for 30 s in a buffered HF solution of 10:1 (H_2O: 37% HF), rinsed in de-ionized water for 10 min, and dried in N_2 (99.999%). Finally, their surfaces were coated by a 2 nm-thick gold catalyst using a Sputter Polaron-SEM Coating System (1 kV, 10 mA).

As indicated in Fig. 1, the source materials were put inside two separate alumina boats. All samples were placed inside alumina boats in the direction of the flow of argon so that the distance between them would be a maximum of 1 cm. Samples A, B and C were placed in the In_2O_3 powder boat while samples D and E were placed in the In_2O_3–graphite powder mix boat, respectively. After placing the samples and boats inside the quartz tube, argon gas was passed through the vacuum tube for 10 min (50 mTorr) to purge atmospheric gases in the media for 10 min (250 mTorr). **When the horizontal tube oven temperature reaches 1000 °C we slowly move the oven and start to experiment.** During the experiment, pressure inside the tube increased from 250 mTorr to 2 Torr due to the presence of graphite powder but decreased again to 250 mTorr after 15 min. Violet, yellowish-blue, salmon and yellowish-green colorations were observed in samples cooled to room temperature (taking ~3 h) (Fig. 1).

The structural and morphological analyses of the samples were carried out using an X-ray diffractometer (XRD) technique (PANalytical Empyrean, Cu-K_α, $\lambda = 1.54060$ Å), a field-emission scanning electron microscope (FESEM: FEI Quanta 450 FEG) and a high-resolution transmission electron microscope (FEI Tecnai). In addition, photoluminescence (PL) measurements of the samples were obtained by exciting them at $\lambda = 252$ nm and $\lambda = 420$ nm wavelengths (Shimadzu RF-5301PC Spectrofluorophotometer) with a 150 W Xenon lamp at RT.

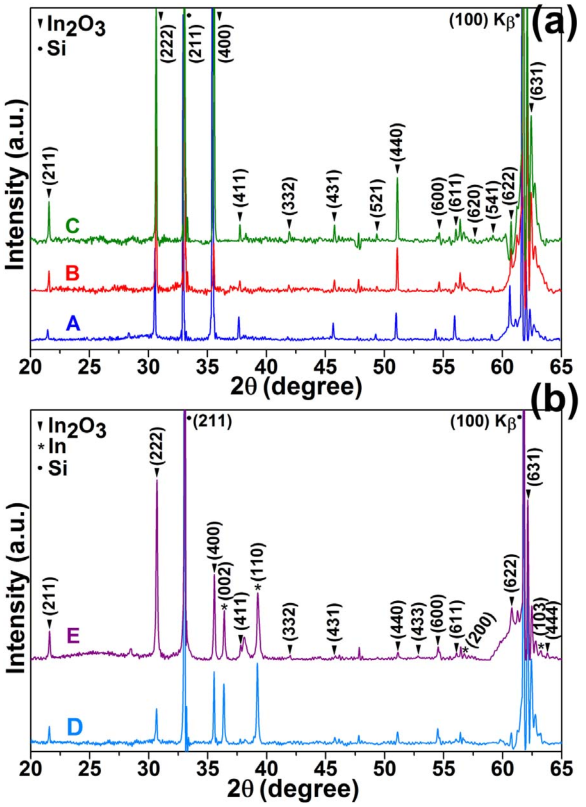

Fig. 2. XRD patterns of (a) A, B and C samples (b) D and E samples.

3. Results and discussion

XRD patterns of all samples obtained at 2θ values between 20° and 65° are shown in Fig. 2(a–b). All samples, based on JCPDS Card No: 06–0416, have diffraction peaks belonging to the (211), (222), (400), (411), (332), (431), (440), (600), (611), (622) and (631) crystal planes of the body-centered cubic (BCC) crystal structure of In_2O_3 with a lattice constant of a = 10.12 Å. Moreover, diffraction peaks belonging to the (521), (620) and (541) crystal planes of In_2O_3 are present only in samples A, B and C, while those belonging to the (433) and (444) crystal planes are present only in samples D and E. Another difference between samples D and E compared to samples A, B and C is that, based on JCPDS Card No: 05–0642, the diffraction peaks belonging to the (002), (110), (200) and (103) crystal planes of the tetragonal crystal structure of indium are present only in samples D and E. This is because in samples D and E nanotowers formed as a result of reactions indicated in Eqs. (1) and (2). In the high-temperature case, Eq. (1) indicates the formation of indium vapor and carbon monoxide (CO) due to the carbothermal reduction reaction between In_2O_3 and the graphite powders, while Eq. (2) shows that indium vapor reacting with oxygen present in the ambient environment, forming In_2O_3.

$$In_2O_3(s) + 3C(s) \rightarrow 2In(v) + 3CO(g) \tag{1}$$

$$4In(v) + 3O_2(g) \rightarrow 2In_2O_3(s) \tag{2}$$

Elemental analyses of all samples—except sample B—were performed with an EDS analyzer in the FESEM system (EDAX, AMETEK Materials Analysis Division). HR-TEM analysis was performed by putting a tiny drop of suspension—formed by ultrasonic dissolution of sample D in 1–2 ml of ethanol for 5–10 s—on a TEM grid.